Available online at www.sciencedirect.com
ScienceDirect
Journal of Organometallic Chemistry 693 (2008) 1552–1563
Journal of Organometallic Chemistry
www.elsevier.com/locate/jorganchem

Density functional study of the complete pathway for the Heck reaction with palladium diphosphines

Panida Surawatanawong, Yubo Fan, Michael B. Hall *

Department of Chemistry, Texas A&M University, P.O. Box 30012, College Station, TX 77843, United States

Received 28 September 2007; received in revised form 16 January 2008; accepted 16 January 2008
Available online 26 January 2008

Dedicated to the memory of Professor F. Albert Cotton, a truly inspiring colleague

Abstract

The reaction mechanism for the complete catalytic cycle of the Heck reaction (between phenyl bromide, C_6H_5Br, and ethylene, C_2H_4, in the presence of the base, NEt_3 to form the product styrene, C_6H_5–C_2H_3), catalyzed by diphosphinopalladium complexes, $Pd(PR_3)_2$ {R = H, Me, Ph}, was investigated by using density functional theory (DFT). The relative free energies of the fully-optimized species in gas phase at 298.15 K and 1 atm were corrected for solvation in DMSO at 1 mol/L by using conductor-like polarizable continuum model (CPCM). The calculations indicate a four-step mechanism for the catalysis, including oxidative addition of C_6H_5Br, migratory insertion of C_6H_5 to C_2H_4, β-hydride transfer/olefin elimination of product, and catalyst regeneration by removal of HBr. Our calculations demonstrate that Pd π-complexes can be formed with phenyl bromide and ethylene before the oxidative addition occurs. Subsequently, various reaction paths were studied for the oxidative addition of phenyl bromide to palladium complexes, coordinated by phosphine(s) and/or ethylene. Interestingly, all pathways lead to palladium monophosphine as the active catalyst. Careful exploration was made on two possible pathways for the migratory insertion and β-hydride-transfer/olefin elimination: (1) the neutral path with bromide bound to Pd and (2) the cationic path with prior bromide ion dissociation. The neutral path is preferred to the cationic path, especially when the more bulky phosphines such as triphenylphosphine are involved.

Keywords: Heck reaction; Palladium; Phosphine; Density functional; Theoretical; Oxidative addition

1. Introduction

The Heck reaction, one of the most utilized cross-coupling reactions, is the palladium-catalyzed arylation of an olefin with an aryl halide under basic conditions (Scheme 1). Since its independent discovery in the early 1970s by Heck [1] and Misoroki [2], the Heck reaction has been widely used as a tool for organic synthesis because of its importance in the direct attachment of olefinic groups to aromatic rings [3–11]. Numerous review articles on various aspects of the Heck and other cross-coupling reactions with palladium catalysts have been published [10–22]. Many types of ligands have been explored for the palladium catalysts in the Heck reaction, e.g., phosphine [1,23–28], carbene [29,30], amine [31] and thiolate [32]. Even a "ligand-free" system has been shown to function well [33,34]. Among these different ligands, the phosphines; especially, the monodentate ones are still the most widely used [3–9].

The traditional mechanism [20,22] for the reaction is well known (Scheme 2). The oxidative addition of organic halide (RX) to the palladium(0) catalyst (Pd^0L_2) generates a *cis*-$RPd^{II}XL_2$ complex. Then, the olefin coordinates to Pd and inserts into the Pd–R bond by a migratory insertion mechanism. A new substituted alkene is produced and released by β-hydride transfer/olefin-elimination. Finally, a base removes HX to regenerate the active Pd complex. The oxidative addition is considered as a key step of the

* Corresponding author.
E-mail addresses: panidasu@mail.chem.tamu.edu (P. Surawatanawong), yubofan@mail.chem.tamu.edu (Y. Fan), mbhall@tamu.edu (M.B. Hall).

0022-328X/$ - see front matter © 2008 Elsevier B.V. All rights reserved.
doi:10.1016/j.jorganchem.2008.01.034

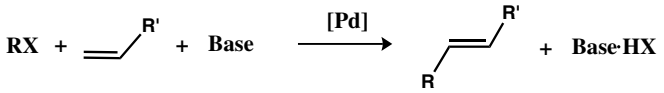

Scheme 1. Heck reaction. (R = aryl).

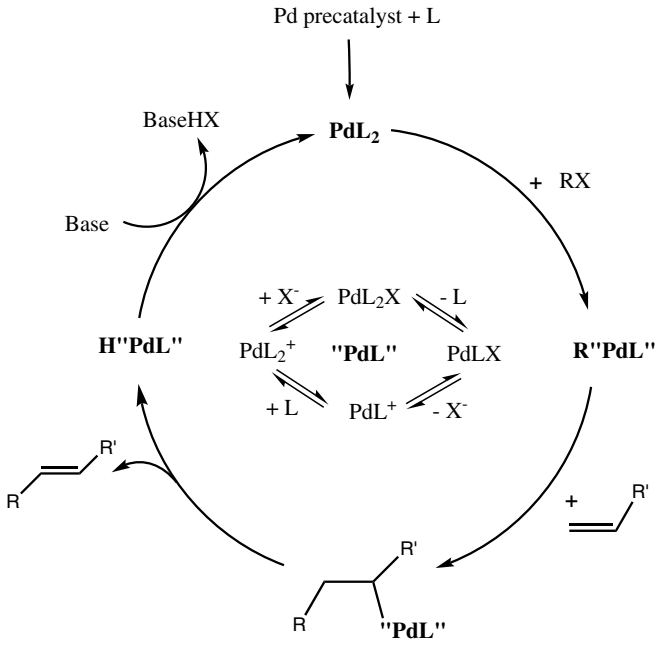

Scheme 2. Traditional Heck reaction mechanism. ("PdL" could be any of the four species that are shown above).

reaction cycle [35]. For monodentate phosphine ligands, the palladium diphosphines were believed to be the active species, with which the aryl halides undergo oxidative addition [22,36,37]. Recently, there has been more evidence for palladium monophosphines as the active catalysts [14,18]. In a study of Suzuki coupling, Littke et al. showed that 1:1 and 1:1.5 ratios of Pd:P gave higher catalytic activity than the 1:2 ratio [38]. Furthermore, Hartwig and coworkers isolated a series of T-shaped three-coordinated palladium compounds [Pd(Ph)(X)(PR_3)] [39,40], which confirmed the existence of intermediate monophosphine palladium species. Another concern at this step of the reaction is that the olefin can also bind to the palladium catalyst. By forming a π-complex before the oxidative addition of aryl halides, high olefin concentrations can slow down the reaction due to the competition between the olefin and the aryl halide for the vacant site in the active palladium species [41,42].

After the oxidative addition, the reaction proceeds through the migratory insertion and β-hydride transfer/olefin-elimination steps. From kinetic studies, the associative mechanism of olefin insertion via a five-coordinate intermediate is unlikely [43–45]. In the dissociative mechanism there are two possible pathways: [22]: (i) a neutral pathway via the dissociation of one phosphine ligand and, (ii) a cationic pathway via the dissociation of the halide ligand. With phenyl halides as substrates and phosphines as ligands, the dissociation of phosphine is more likely because of the weaker Pd–P bond relative to the Pd–X bond [46]. It is important to point out that the reaction can switch from one pathway to the other when the reaction conditions change [47].

Key steps in the mechanism for Pd-mediated cross-coupling reactions, including the Heck reaction, have been studied by theory [46,48,49], especially the oxidative addition of aryl halides to palladium complexes. In early studies, only oxidative additions to palladium diphosphines were considered [50–52] until Ahlquist et al. concluded that monophosphines were important as the major contribution to the reaction barriers arises from phosphine dissociation [53,54]. The insertion and elimination steps for the Heck reaction have also been studied. Roesch and coworkers found that the cationic pathway is preferred for carbene ligands because of the stronger Pd–C bond relative to the Pd–halide bond [48]. Assuming the neutral pathway, Guo and coworkers studied the full catalytic cycle of the Heck coupling by comparing palladium to nickel complexes with PH_3 as model ligands and vinyl halides as substrates [46]. Sundermann et al. studied the Pd(II)/Pd(IV) mechanism by the oxidative addition of phenyl iodide to palladium(II) bidentate phosphine complexes leading to octahedral Pd(IV) complexes [49]. Although the overall free energy barriers in the oxidative addition step for Pd(II)/Pd(IV) is significantly larger than that for Pd(0)/Pd(II), they concluded that olefin binding and iodide dissociation result in more difficult oxidative addition via Pd(0)/Pd(II) than Pd(II)/Pd(IV).

Although sterically hindered ligands are used in the reaction, the catalytic cycle of the Heck reaction were computed using over-simplified or truncated ligands and substrates, such as small phosphine ligands (PH_3 or PMe_3) and vinyl halides (instead of aryl halides). For experimentally used phosphines, only the oxidative addition step has been studied [53,54]. Moreover, the Heck reaction cycle actually involves several possible pathways; previous calculations covered some of these aspects but not all of them. To the best of our knowledge, complexities, such as solvent effects, the size of PR_3 ligands and competing pathways in the catalytic cycle of the Heck reaction, have not been studied theoretically. Here, we calculate the pathways in the oxidative addition of phenyl bromide to palladium complexes with diphosphine, monophosphine and/or olefin as alternative ligands. In the migratory insertion, β-hydride transfer/olefin elimination, and catalyst recovery, both neutral and cationic pathways were calculated. The experimental phosphine ligands (PPh_3) were used and compared with the model phosphine ligands (PH_3 and PMe_3) throughout the reaction.

2. Computational details

All calculations were performed with the GAUSSIAN03 program package [55]. The density functional, PBE [56], was used for geometry optimization with modified LANL2DZ+f basis set for Pd, LANL2DZdp for P and

Br atoms with effective core potentials (ECP) [57–59], 6-31++G(d′,p′) [60–62] for C and H atoms except for those on the phosphine's phenyl rings, where we use 6-31G(d) [60–62]. Geometry and frequency calculations were performed with the PBE functional because the density fitting procedure increases the speed of these calculations. Previous work [63] has shown that the B3LYP energies are similar to CCSD(T) for CH_4 oxidative addition to Pd. Our own test calculations showed less than 1 kcal/mol between B3LYP//PBE and all B3LYP calculations. Therefore, single point energies were recalculated with the B3LYP functional [64,65] using the same basis set. All structures were fully optimized with default convergence criteria, and frequencies were calculated to ensure that there are no imaginary frequencies for minima and only one imaginary frequency for transition states. Zero point energies and thermodynamic functions were calculated at 298.15 K and 1 atm. The B3LYP solvation energies were calculated on the geometries from PBE gas-phase optimizations by using CPCM [66,67] method with UAKS atomic radii and solvation parameters corresponding to DMSO ($\varepsilon = 46.7$). By using B3LYP//PBE/6-31G(d) method with CPCM model and UAKS atomic radii, test calculation of the solvation free energy of CH_3NH_3 and *N*-methylacetamide, in which the experimental solvation energies are available [68], gave an error of less than 1 kcal/mol. The standard states were corrected to 1 mol/L (see Supporting information for standard state conversion). The free energies and enthalpies shown in all figures and tables are relative to $Pd(PR_3)_2 + PhBr + C_2H_4 + NEt_3$.

3. Results and discussion

The results for the reaction pathway for $Pd(PR_3)_2$ catalyst with phenyl bromide and ethylene by density-functional theory combined with continuum solvation model are presented below beginning with an energy comparison for three possible pathways of the oxidative addition, and then the migratory insertion of the ethylene, the β-hydride transfer/olefin elimination of the product styrene, and the abstraction of proton by the NEt_3 base. The B3LYP relative enthalpies, gas-phase free energies and free energies with solvent correction of all involving species are shown in Tables 1 and 2 (The relative enthalpies and free energies from PBE calculation are in Supporting information). Unless specified otherwise, the free energies throughout the article refers to the B3LYP free energies with solvent correction. The relative free energies of the corresponding structures for different phosphine ligands were compared throughout.

3.1. The oxidative addition

In early studies of the Heck reaction, the phenyl bromide was believed to undergo oxidative addition on palladium diphosphine $Pd(PR_3)_2$ Eq. (1) [22,36,37]. Later, some workers found that ethylene can also coordinate to $Pd(PR_3)_2$ quite easily [41,42]; therefore, we also examined the oxidative addition of phenyl bromide on $Pd(PR_3)(\eta^2\text{-}C_2H_4)$ Eq. (2). Recently, more evidence has accumulated that phosphine dissociation from $Pd(PR_3)_2$ occurs before the oxidative addition [14,18] Eq. (3). We will discuss each of these pathways in this section.

$$Pd(PR_3)_2 + PhBr \rightarrow Pd(PR_3)_2(Br)(Ph) \quad (1)$$

$$Pd(PR_3)(\eta^2\text{-}C_2H_4) + PhBr \rightarrow Pd(PR_3)(\eta^2\text{-}C_2H_4)(Br)(Ph) \quad (2)$$

$$Pd(PR_3) + PhBr \rightarrow Pd(PR_3)(Br)(Ph) \quad (3)$$

3.1.1. The oxidative addition to palladium diphosphine

First, we consider phenyl bromide undergoing oxidative addition directly to the palladium diphosphine. The optimized geometry of $Pd(PR_3)_2$ (**1**) is nearly linear [69]. The Pd–P bond lengths are 2.29, 2.31, and 2.32 Å for R = H, Me, and Ph (Fig. 1), respectively; the bond lengths increase slightly with the size of ligands (see Supporting information for full geometric parameters). A π-complex, **17**, of the aryl halide with the palladium catalyst is believed to form

Table 1
The B3LYP relative enthalpies, gas-phase free energies, and free energies with solvent correction of palladium complexes in the oxidative addition

	ΔH (1 atm)			ΔG_{gas} (1 atm)			ΔG_{Total} (1 M)		
	PH_3	PMe_3	PPh_3	PH_3	PMe_3	PPh_3	PH_3	PMe_3	PPh_3
1	0.00	0.00	0.00	0.00	0.00	0.00	0.00	0.00	0.00
17	5.78	8.60	5.52	16.30	22.10	17.90	16.52	25.91	27.79
2-TS	13.95	16.64	15.36	25.00	29.38	27.81	25.00	33.46	35.77
3	−13.11	−16.97	−5.30	−1.45	−4.59	8.57	−5.62	−8.09	10.50
29	−10.05	−6.93	−7.75	0.42	5.18	3.10	−2.22	4.53	5.22
19	1.94	7.39	7.49	2.96	6.82	4.13	2.56	2.32	−2.40
20	6.19	13.13	11.08	18.44	25.82	20.56	17.57	22.55	18.49
21-TS	16.60	23.05	21.26	29.20	35.57	32.07	28.01	32.93	29.48
22	−0.50	2.41	5.26	12.07	14.37	15.36	7.81	6.82	7.31
6	25.15	29.85	31.53	16.94	20.29	18.87	18.63	17.37	13.07
18	11.76	17.23	16.12	11.04	17.31	15.34	12.99	16.15	12.89
7-TS	18.51	23.43	22.24	20.09	24.46	22.72	22.37	23.39	20.99
8	1.50	1.72	2.17	2.55	2.22	1.82	1.21	−3.55	−3.91

Table 2
The B3LYP relative enthalpies, gas-phase free energies, and free energies with solvent correction of palladium complexes in the migratory insertion, β-H transfer/olefin elimination and catalyst recovery

	ΔH (1 atm)			ΔG_{gas} (1 atm)			ΔG_{Total} (1 M)		
	PH_3	PMe_3	PPh_3	PH_3	PMe_3	PPh_3	PH_3	PMe_3	PPh_3
Neutral path									
Migratory insertion									
8	1.50	1.72	2.17	2.55	2.22	1.82	1.21	−3.55	−3.91
8b	10.76	13.08	13.22	10.35	12.42	9.87	10.81	9.64	6.51
22	−0.50	2.41	5.26	12.07	14.37	15.36	7.81	6.82	7.31
23-TS	6.19	7.33	10.32	20.40	20.11	21.94	15.28	12.11	13.21
β-H transfer/olefin elimination									
24	−18.45	−20.39	−18.96	−5.45	−7.73	−9.18	−10.58	−15.51	−17.45
25-TS	−10.99	−9.52	−8.36	2.56	3.87	2.55	−2.44	−3.82	−5.32
26	−14.05	−9.13	−8.05	−1.07	2.69	2.50	−5.06	−4.42	−2.73
Catalyst recovery									
27	−6.64	−7.08	−6.97	−6.91	−7.75	−10.34	−9.94	−15.88	−19.85
28	−22.34	−15.75	−18.80	−8.98	−2.27	−7.88	−15.96	−11.45	−16.00
31	105.24	109.94	111.63	101.62	104.98	103.56	−3.77	−5.02	−9.32
30	80.09	80.09	80.09	84.69	84.69	84.69	−22.39	−22.39	−22.39
Cationic path									
Migratory insertion									
8	1.50	1.72	2.17	2.55	2.22	1.82	1.21	−3.55	−3.91
3	−13.11	−16.97	−5.30	−1.45	−4.59	8.57	−5.62	−8.09	10.50
4	106.86	88.65	82.94	110.59	92.25	87.01	16.10	3.55	10.89
5	94.05	84.40	82.63	109.50	101.66	102.30	11.70	8.71	22.52
11-TS	99.64	88.73	86.39	115.86	107.64	106.91	18.62	14.92	27.36
β-H transfer/olefin elimination									
12	78.14	62.40	55.31	93.17	79.67	72.16	−3.69	−10.31	−5.28
13-TS	81.01	66.76	59.99	96.25	84.55	77.35	−0.08	−5.89	0.06
14	80.82	66.77	59.47	95.41	83.53	77.03	−0.19	−6.19	0.26
Catalyst recovery									
15	100.58	75.82	66.13	101.85	78.00	65.24	2.08	−14.15	−16.63
16	63.84	59.21	46.62	79.57	75.78	62.15	−12.56	−8.65	−12.24
30	80.09	80.09	80.09	84.69	84.69	84.69	−22.39	−22.39	−22.39

before the oxidative addition [46,70]. The Pd–C(11) bonds are slightly shorter than Pd–C(18) bonds because the bromide, an electron-withdrawing group, is attached to C(11). The formation of **17** increases the free energy by 16.52, 25.91, and 27.79 kcal/mol for R = H, Me, and Ph (Table 1), respectively. The entropy disfavors this associative reaction and the relative gas-phase enthalpies (Table 1) are also positive.

The free energies of the transition states for the oxidative addition, **2-TS**, are 25.00, 33.46, and 35.77 kcal/mol for R = H, Me, and Ph. The higher free energies correspond to larger P–Pd–P angles of 110.9°, 119.4°, and 127.1° for R = H, Me, and Ph, respectively, and larger dihedral angles [C(11)–Br(10)–Pd(1)–P(2)] of 66.4°, 69.1°, and 85.0°. The most sterically hindered phosphines are the most deformed from square planar. Strikingly, the free energy difference between the transition states **2-TS** and the π-complexes **17** is ~8 kcal/mol for all phosphine ligands. In the study by Toro-Labbe and coworkers, following the reaction force as a function of reaction coordinate, the structural reordering from reactant to transition state takes place in the early stage of the reaction coordinate [71]. The difference in the free energy of **2-TS** for different phosphine ligands depends mainly on the energetic cost of distorting the linear structures.

The products from the oxidative addition are $Pd(PR_3)_2$-(Ph)(Br) (**3**) with two *cis*-phosphines. The Pd–P(3) bond *trans* to the phenyl is ~0.12 Å longer than the Pd–P(2) bond *trans* to the bromide due to the strong *trans* effect of the phenyl. The Pd–Br and Pd–C(11) are ~0.10 Å shorter than those in **2-TS** as these bonds are fully formed in **3**. The steric effect from ligands appears more strongly in **3** than **2-TS**: (i) the σ-bound phenyl ring of **3** is nearly perpendicular to the palladium coordination plane for PH_3 and PMe_3 with dihedral C(18)–C(11)–Pd(1)–Br(10) angles of 89.8° and 87.3°, respectively, but the phenyl ring tilts to make a dihedral angle of 68.9° for PPh_3; and (ii) the *cis*-complexes **3** are square-planar structures for PH_3 and PMe_3 with dihedral C(11)–Br(10)–Pd(1)–P(2) angles of −0.2° and 1.1°, respectively, but for PPh_3 the square-planar structure is significantly distorted with a dihedral angle of 57.9°. Correspondingly, the relative free energies of **3** are −5.62, −8.09, and 10.50 kcal/mol for R = H, Me, and Ph, respectively.

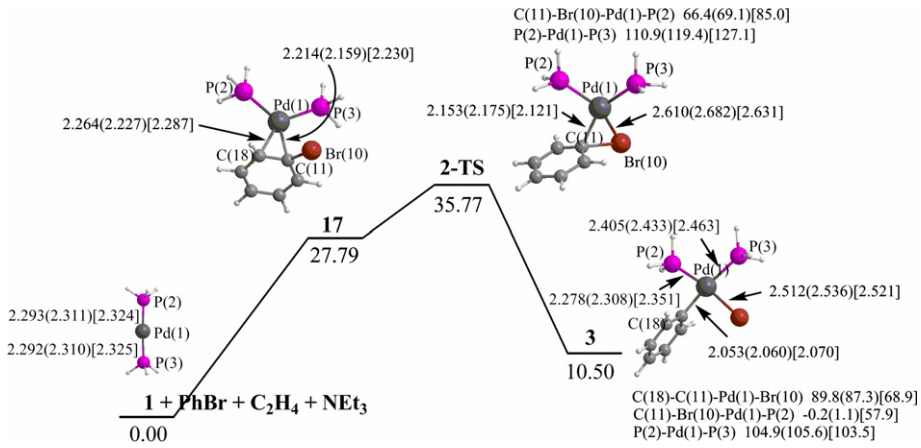

Fig. 1. Free energy profiles for the oxidative addition to palladium diphosphine. The relative free energies in DMSO solution for PPh_3 are given in kcal/mol. Calculated bond distances and angles for PH_3, PMe_3 (in parentheses), and PPh_3 (in brackets) are given in Å and °. To simplify the figure, only the structures for PH_3 are shown.

3.1.2. The oxidative addition to ethylene-coordinated palladium monophosphine

In the reaction system, a π-complex of palladium diphosphine can be formed not only with phenyl bromide but also ethylene. Ethylene actually binds more strongly than phenyl bromide. The Pd–C bonds in $Pd(PR_3)_2(\eta^2\text{-}C_2H_4)$ (**29**) are shorter than the ones in **17** (Figs. 1 and 2) and the free energies of **29** are significantly lower than **17** (Table 1). Amatore et al. suggested that the olefin coordination at this step decreases the reaction rate through the equilibrium $\mathbf{1} + C_2H_4 \rightleftharpoons \mathbf{29}$, which reduces the concentration of **1** [42]. However, what if the π-complex of palladium diphosphine with the olefin proceeds to the oxidative addition with the phenyl bromide? How high is this free energy barrier?

Prior to oxidative addition, the dissociation of one phosphine from complex **29** creates $Pd(PR_3)(\eta^2\text{-}C_2H_4)$ (**19**) with a free energy increase for PH_3 but decreases for PMe_3 and PPh_3 (Table 1). Complex **19** is similar to **1** in that the palladium center coordinates to two ligands but with the ethylene replacing one phosphine ligand; the π-donor and π^*-acceptor in the ethylene play the same role in stabilizing Pd as the lone-pair donor and σ^*-acceptor in the phosphine. Again, a phenyl bromide π-complex, $Pd(PR_3)(\eta^2\text{-}C_2H_4)(\eta^2\text{-}PhBr)$ (**20**), precedes the oxidative addition (Fig. 2). For PH_3 and PMe_3 ligands, both π-complexes **20** and **17** are comparable in free energies while for PPh_3 ligands, complex **20** is 9.3 kcal/mol lower in free energy than **17** (Table 1, Figs. 1 and 2). The same situation applies to the comparison of the free energies between the oxidative addition transition-states **21-TS** and **2-TS**. The results show that the replacement of one phosphine ligand by the ethylene is favorable for the oxidative addition of palladium complexes with the sterically-hindered ligands such as PPh_3.

3.1.3. The oxidative addition to palladium monophosphine

Monoligated palladium species have been proposed to be important intermediates in the catalytic cycle [14,18]. The isolation of three-coordinate palladium compounds, $[Pd(PR_3)(Ph)(X)]$, with T-shaped geometries support the possibility of this pathway [39,40]. Thus, we examined phosphine dissociation from palladium diphosphine prior to the oxidative addition of the phenyl bromide. The Pd–P(2) bond in $PdPR_3$ (**6**) is 0.1 Å shorter than the one in $Pd(PR_3)_2$ (Fig. 3); the shortened bond compensates, in part, for the loss of one metal–ligand bond. Importantly, the solvation contributes to this dissociation because both PR_3 and $Pd(PR_3)$ are polar molecules, while $Pd(PR_3)_2$ is not; with solvent correction, the relative free energies are less than the relative gas phase free energies by 2.92 and 5.80 kcal/mol for PMe_3 and PPh_3. The calculations predict that more sterically-hindered ligands dissociate more easily; the dissociation free energies are 18.63, 17.37, and 13.07 kcal/mol for PH_3, PMe_3, and PPh_3, respectively (Fig. 3 and Table 1). Ahlquist et al. reported that $Pd(PPh_3)(DMF)$ is more stable than $Pd(PPh_3)$ by −4.54 kcal/mol in the gas phase [54]. In strongly coordinating solvents, the monophosphine palladium, $PdPR_3$, species could bind to DMSO and form some $Pd(PR_3)(DMSO)$ in equilibrium with $PdPR_3$.

The monophosphine π-bound complexes of phenyl bromide, $Pd(PR_3)(\eta^2\text{-}PhBr)$ (**18**), are formed with lower free energies than the more crowded π-bound complexes **17** and **20** (Table 1). Likewise, for the oxidative addition of phenyl bromide via transition state **7-TS**, the free energies of activation are lower than those of **2-TS** and **21-TS** for the corresponding phosphine ligands. Interestingly, the free energies of the **7-TS** are actually similar for all phosphine ligands; the main difference from different phosphine ligands is in the phosphine dissociation step. The **7-TS** structure has small ~52° C(11)–Pd–Br angles (Fig. 3) as expected for an early transition state. Following transition state **7-TS** the system rearranges to the T-shaped structure $Pd(PR_3)(Ph)(Br)$ (**8**), where the C(11)–Pd–Br angle ranges from 98° to 105° and the Pd–Br and Pd–C(11) bonds are shorter (Fig. 3) than the ones in **7-TS**; the relative free energies of **8** are 1.21, −3.55, and −3.91 kcal/mol for PH_3, PMe_3, and PPh_3, respectively. These latter structures (**8**)

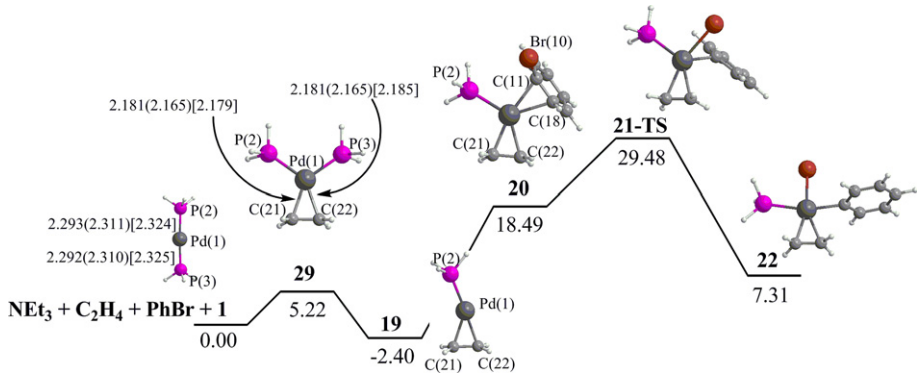

Fig. 2. Free energy profiles for the oxidative addition to ethylene-coordinated palladium monophosphine. The relative free energies in DMSO solution for PPh_3 are given in kcal/mol. Calculated bond distances for PH_3, PMe_3 (in parentheses), and PPh_3 (in brackets) are given in Å.

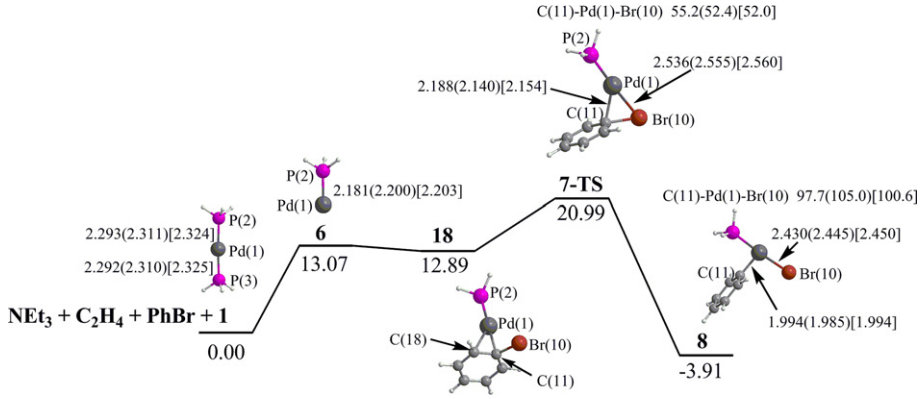

Fig. 3. Free energy profiles for the oxidative addition to palladium monophosphine. The relative free energies in DMSO solution for PPh_3 are given in kcal/mol. Calculated bond distances and angles for PH_3, PMe_3 (in parentheses), and PPh_3 (in brackets) are given in Å and °.

are similar to those observed [39,40] and in both **7-TS** and **8** the bromide and the phosphine are *trans* to each other and phenyl group is *trans* to the empty site because the latter has the largest *trans* influence.

3.1.4. The probable oxidative addition pathway

The three pathways described above actually intersect as all three are connected by phosphine and ethylene association and dissociation (Scheme 3). The rate determining barrier for the oxidative addition is lowest at the monophosphine **7-TS**. Although the ethylene can form π-coordinated palladium diphosphine effortlessly, the oxidative addition to palladium with ethylene attached is unlikely due to the high barrier. However, the ethylene-coordinating palladium complex $Pd(PR_3)_2(\eta^2\text{-}C_2H_4)$ (**29**) can lose one phosphine (leading to **19**) and later lose ethylene to become palladium monophosphine **6** which can proceed to the oxidative addition through **7-TS** (Scheme 3).

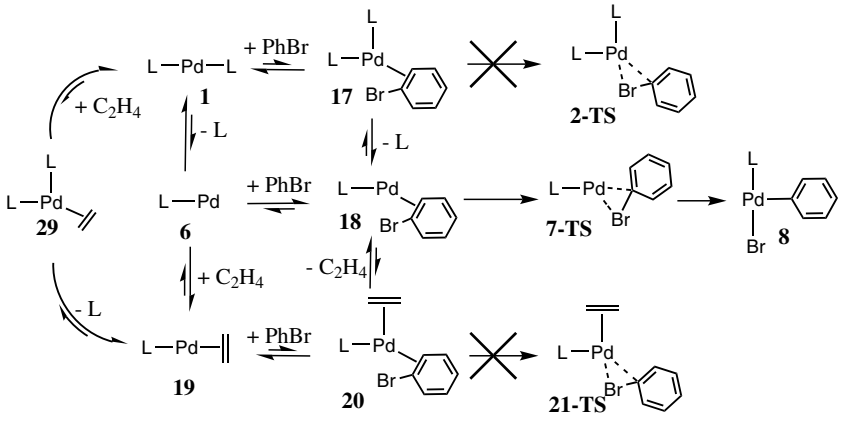

Scheme 3. The equilibrium species prior to the oxidative addition (L = phosphine).

Similarly, when the phenyl bromide forms a π-complex with palladium diphosphine (leading to **17**), one phosphine can dissociate to generate $Pd(PR_3)(\eta^2\text{-PhBr})$ (**18**), which can proceed to the oxidative addition through **7-TS**. According to our calculation, all of the possible pathways lead to palladium monophosphine as the active species that breaks the Ph–X bond in the oxidative addition step.

3.2. The migratory insertion, β-hydride transfer/olefin elimination and catalyst recovery

For the remaining reaction steps: the migratory insertion of ethylene, the β-hydride transfer/olefin-elimination of the product styrene and the abstraction of proton by the base NEt_3, we examined two possible pathways: (i) neutral pathway – the olefin binds to a three-coordinated neutral species with one phosphine, one bromide, and one phenyl ligand Eq. (4); and (ii) cationic pathway – the olefin binds to three-coordinate cationic (1+) species with two phosphines and one phenyl ligand Eq. (5). We will compare and discuss both pathways for each step of the reaction.

$$Pd(PR_3)(Br)(Ph) + C_2H_4 \rightarrow Pd(PR_3)(Br)(Ph)(\eta^2\text{-}C_2H_4) \quad (4)$$

$$[Pd(PR_3)_2(Ph)]^+ + C_2H_4 \rightarrow [Pd(PR_3)_2(Ph)(\eta^2\text{-}C_2H_4)]^+ \quad (5)$$

3.2.1. The migratory insertion

In the neutral pathway, $Pd(PR_3)(Ph)(Br)$ (**8**) with the phenyl *trans* to the vacant site rearranges to **8b** with the bromide *trans* to the vacant site (Fig. 4a). The free energy increases for **8b** because the phenyl with the high *trans* influence moves *trans* to phosphine, which weakens the Pd–P bond; the Pd–P in **8b** is longer by ~0.14 Å relative to that in **8**. The ethylene then binds to the vacant site of **8b** to form η^2-ethylene complex $Pd(PR_3)(Ph)(Br)(\eta^2\text{-}C_2H_4)$ (**22**). The square planar four-coordinated structure of **22** is slightly more stable than the T-shaped three-coordinated structure **8b** for PH_3 and PMe_3 ligands by ~3 kcal/mol but less stable for PPh_3 by 0.8 kcal/mol (Table 2). Species **22** lead to transition states **23-TS** with the C(11) from phenyl close to C(22) from ethylene (Fig. 4a). In **23-TS**, C(11)–C(22) distance is about 0.5 Å shorter and the ethyl-

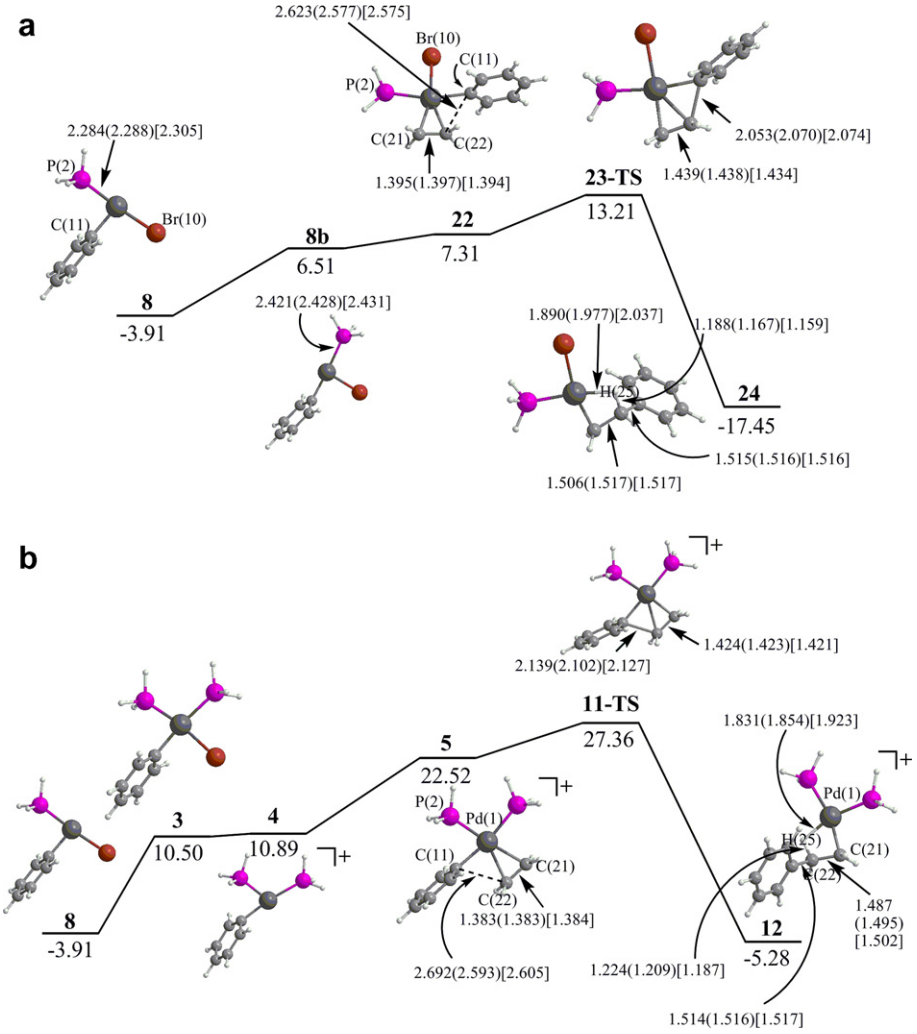

Fig. 4. Free energy profiles for the migratory insertion in: (a) the neutral pathway and (b) the cationic pathway. The relative free energies in DMSO solution for PPh_3 are given in kcal/mol. Calculated bond distances for PH_3, PMe_3 (in parentheses), and PPh_3 (in brackets) are given in Å.

ene bond, C(21)–C(22), is about 0.04 Å longer than those in **22**. The free energy barriers relative to **22** are 7.47, 5.29, and 5.90 kcal/mol for PH_3, PMe_3, and PPh_3, respectively.

When the phenyl ring completes the migration from the metal to the ethylene, the intermediate species (**24**) has an agostic Pd–H(25) bond (Fig. 4a). Compared with **23-TS**, the C(11)–C(22) bond lengths in **24** are shortened to ~1.51 Å, consistent with a C–C single bond (1.47 Å in free styrene from a PBE calculation in the same basis set). Moreover, the C(22)–C(21) bond distances are lengthened to a single bond at ~1.51 Å. The agostic hydrogen H(25) results in longer C(22)–H(25) bond lengths (1.19, 1.17, and 1.16 Å for PH_3, PMe_3 and PPh_3) and close Pd–H(25) contacts (1.90, 1.98, and 2.04 Å for PH_3, PMe_3 and PPh_3). The formation of the new C–C bond makes the formation of **24** exergonic by −10.58, −15.51, and −17.45 kcal/mol for PH_3, PMe_3, and PPh_3, respectively. In complexes **24** larger ligands (PR_3) correlated with the stronger C–H bond and weaker agostic interactions.

In the gas phase, reactions involving charged-separation processes are difficult and the corresponding gas-phase enthalpies and free energies of **4** and all other cationic species are very high relative to neutral species (Table 2). However, in polar solvent, these charge species are stabilized; thus, solvation (and appropriate solvent correction) is important to compare the free energies between neutral and cationic species.

In the cationic pathway, the phosphine ligand binds to $Pd(PR_3)(Ph)(Br)$ (**8**) to form $Pd(PR_3)_2(Ph)(Br)$ (**3**), then bromide ion dissociates from the palladium center, leading to $[Pd(PR_3)_2(Ph)]^+$ (**4**), and the ethylene binds at the vacant site, forming $[Pd(PR_3)_2(Ph)(\eta^2\text{-}C_2H_4)]^+$ (**5**) (Fig. 4b). The square-planar four-coordinate structure **5** is more stable than the T-shaped three-coordinate structure **4** by −4.40 kcal/mol for PH_3, but less stable by 5.16 and 11.63 kcal/mol for PMe_3 and PPh_3 (Fig. 4b and Table 2). Then $[Pd(PR_3)_2(Ph)(\eta^2\text{-}C_2H_4)]^+$ (**5**) leads to the transition state **11-TS**; like **23-TS** in the neutral path, the C(11) from phenyl comes close to the C(22) in the ethylene while the C–C double bond in the ethylene is elongated in the migration process (Fig. 4b). **11-TS** leads to the intermediate species **12** with an agostic bond interaction, like that in the neutral species **24**. For all phosphine ligands we studied, the free energy profiles of the cationic pathway lie above the neutral pathway for the migratory insertion step.

The cationic pathway is complicated by some additional issues. Experimentally, the *trans* isomer of $Pd(PR_3)_2(Ph)(Br)$ (**3**) is more stable than the *cis*-analog [72]. We also calculated *trans*-$Pd(PR_3)_2(Ph)(Br)$ (**3-trans**) to be lower in energy than the *cis* **3** (PH_3 only). $[Pd(PR_3)_2(Ph)]^+$ (**4**) with two phosphine ligands in the *cis*-position can easily isomerize to **4-trans** which can capture Br^- to form **3-trans** (Fig. 5). The two *trans* isomers are lower in free energy by −4.12 and −2.29 kcal/mol than their *cis*-isomers, respectively. However, to proceed to the migratory insertion step the ethylene has to be *cis* to the phenyl. Thus, **3** and **4** are important intermediates in the cationic pathway but less stable than the unreactive **3-trans** and **4-trans**.

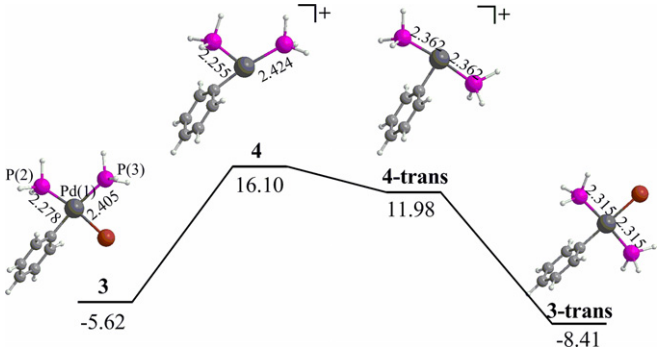

Fig. 5. Free energy profiles for the *cis*/*trans* isomerization. The relative free energies in DMSO solution for PH_3 are given in kcal/mol. Calculated bond distances for PH_3 are given in Å.

3.2.2. The β-hydride transfer/olefin elimination

From the intermediate species **24**, the agostically bound β-hydrogen H(25) transfers from C(22) to palladium via transition state **25-TS** (Fig. 6a). In **25-TS**, the Pd–H(25) bond shortens to 1.59 Å, C(22)–H(25) distance increases to 1.8 Å and the C(21)–C(22) bond shortens to 1.43 Å. The free energy barrier is 8.19, 11.69, and 12.13 kcal/mol for PH_3, PMe_3, and PPh_3, respectively (Table 2).

The intermediate produced through **25-TS**, $Pd(PR_3)(Br)(H)(C_2H_3Ph)$ (**26**), has the C(22)–H(25) bond completely broken. Compared to **24**, the free energies of **26** increase by 5.52, 11.09, and 15.16 kcal/mol for PH_3, PMe_3, and PPh_3, respectively. Finally, styrene is released as product, which leaves $Pd(PR_3)(Br)(H)$ (**27**) in the T-shaped structure with the hydride opposite the empty site. In **27**, the Pd–H bonds are 0.05 Å shorter than those in **26**. The sterically-hindered ligands prefer **27** to **26**, as the free energy changes are −4.88, −11.46, and −17.12 kcal/mol for PH_3, PMe_3, and PPh_3, respectively.

In the cationic pathway, the agostic hydrogen in **12** is transferred from carbon to palladium through transition state **13-TS**. The intermediate formed, $[Pd(PR_3)_2(H)(C_2H_3Ph)]^+$ (**14**), then loses styrene leaving $[Pd(PR_3)_2(H)]^+$ (**15**) in a T-shaped structure with phosphines *trans* to each other and hydride opposite the empty site. Like styrene loss in the neutral pathway **26** → **27**, the sterically-hindered ligand drives styrene loss **14** → **15** with free energy changes of +2.27, −7.96, and −16.89 kcal/mol for PH_3, PMe_3, and PPh_3, respectively.

3.2.3. The recovery of the active catalyst

In order to close the catalytic cycle, a base in the reaction system abstracts the proton from $Pd(PR_3)(Br)(H)$ (**27**) in the neutral pathway and from $[Pd(PR_3)_2(H)]^+$ (**15**) in the cationic pathway. Here, we use NEt_3 as the base. As the nitrogen approaches the proton in **27** to form $Pd(PH_3)(Br)$–$(HNEt_3)$ (**28**), the Pd–H bond is lengthened by ~0.5 Å (Fig. 7a) and the N–H bond distance is

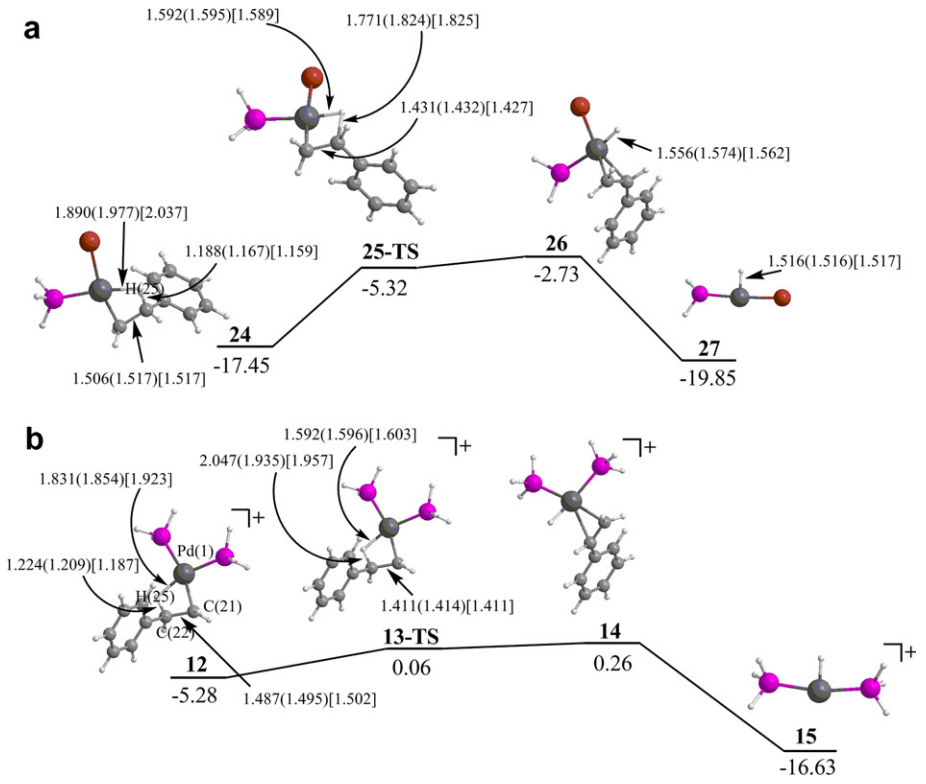

Fig. 6. Free energy profiles for the β-H transfer/olefin elimination in: (a) the neutral pathway and (b) the cationic pathway. The relative free energies in DMSO solution for PPh_3 are given in kcal/mol. Calculated bond distances for PH_3, PMe_3 (in parentheses), and PPh_3 (in brackets) are given in Å.

~1.1 Å. While the formation of the intermediate **28** relative to **27** is favored for PH_3 by −6.02 kcal/mol, its formation for PMe_3 and PPh_3 is disfavored by 4.43 and 3.85 kcal/mol, respectively (Fig. 7a and Table 2). $HNEt_3^+$ and Br^- are eliminated from the palladium center with the free energies increasing by 12.19, 6.43, and 6.68 kcal/mol for PH_3, PMe_3, and PPh_3, respectively. However, when a phosphine ligand binds to regenerate $Pd(PR_3)_2$ in the end, the free energy decreases by −18.62, −17.37, and −13.07 kcal/mol for PH_3, PMe_3, and PPh_3, respectively.

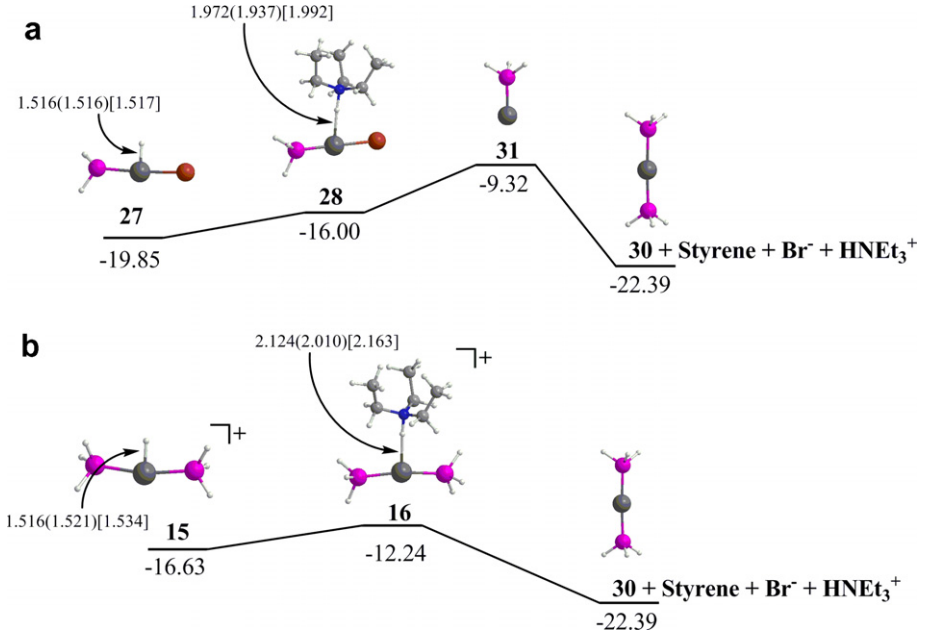

Fig. 7. Free energy profiles for the catalyst recovery in: (a) the neutral pathway and (b) the cationic pathway. The relative free energies in DMSO solution for PPh_3 are given in kcal/mol. Calculated bond distances for PH_3, PMe_3 (in parentheses), and PPh_3 (in brackets) are given in Å.

As in the neutral pathway, NEt_3 abstracts the proton from $[Pd(PH_3)_2(H)]^+$ (**15**) in the cationic pathway to form $[Pd(PH_3)_2(H–NEt_3)]^+$ (**16**) with free energy changes −14.64, 5.50 and 4.39 kcal/mol for PH_3, PMe_3, and PPh_3, respectively (Fig. 7b and Table 2). Finally, dissociation of $HNEt_3^+$ regenerates $Pd(PR_3)_2$ **1** with free energy decreases of −9.83, −13.74, and −10.15 kcal/mol for PH_3, PMe_3, and PPh_3, respectively.

4. Conclusions

By using density functional theory combined with free energy corrections from a continuum solvation calculation, a cycle summarizing the complete reaction was developed (Scheme 4). The highest overall barrier in the catalytic cycle is the oxidative-addition step which is predicted to be the rate-determining step in agreement with experiments. For the oxidative addition to di-ligated palladium, palladium diphosphine and olefin-coordinated palladium monophosphine, the difference in the free energy barrier for different phosphines depends mainly on the energetic cost of distorting the linear structure, whereas for the oxidative addition to palladium monophosphine, the barrier depends mainly on the phosphine dissociation. More sterically-hindered phosphines cause an increasing barrier for the former but a decreasing one for the latter. The solvation contributes mainly to the lower free energy of phosphine dissociation of more sterically-hindered phosphine ligands. Phenyl bromide oxidative addition to palladium monophosphine is the most favorable pathway for all PH_3, PMe_3, and PPh_3 ligands. However, the palladium diphosphine can form π-bound complexes with either ethylene or phenyl bromide before losing one phosphine, or the ethylene, before undergoing the phenyl bromide oxidative addition (Scheme 1). Ziegler and coworkers [50] reported that oxidative addition of phenyl halide on palladium with a bi-dentate phosphine in THF solvent involves the dissociation of halide ion following the oxidative addition before it returns to form the aryl halide complex. For the remaining reaction steps: the migratory insertion, β-H transfer/olefin elimination, and catalyst recovery, the phosphine dissociation leads to neutral pathway and the bromide dissociation leads to cationic pathway. The charged-separation process in the cationic pathway causes very high corresponding gas-phase enthalpies and free energies of all cationic species relative to neutral species; thus, incorporating solvent effect is very important to compare the free energies between neutral and cationic species. Even after these solvation corrections, the neutral pathway is found to lie below the cationic pathway, especially, for the sterically hindered phosphine ligand. The steric hindrance of phosphine ligands affects the free energy barrier particularly in the phosphine dissociation and the stability of four-coordinate structures.

The complexity of the Heck reaction can derive from the fact that there is more than one accessible pathway and different reaction conditions and ligand sets leading the overall reaction to proceed by different paths. Our conclusions apply primarily to palladium monodentate–phosphine

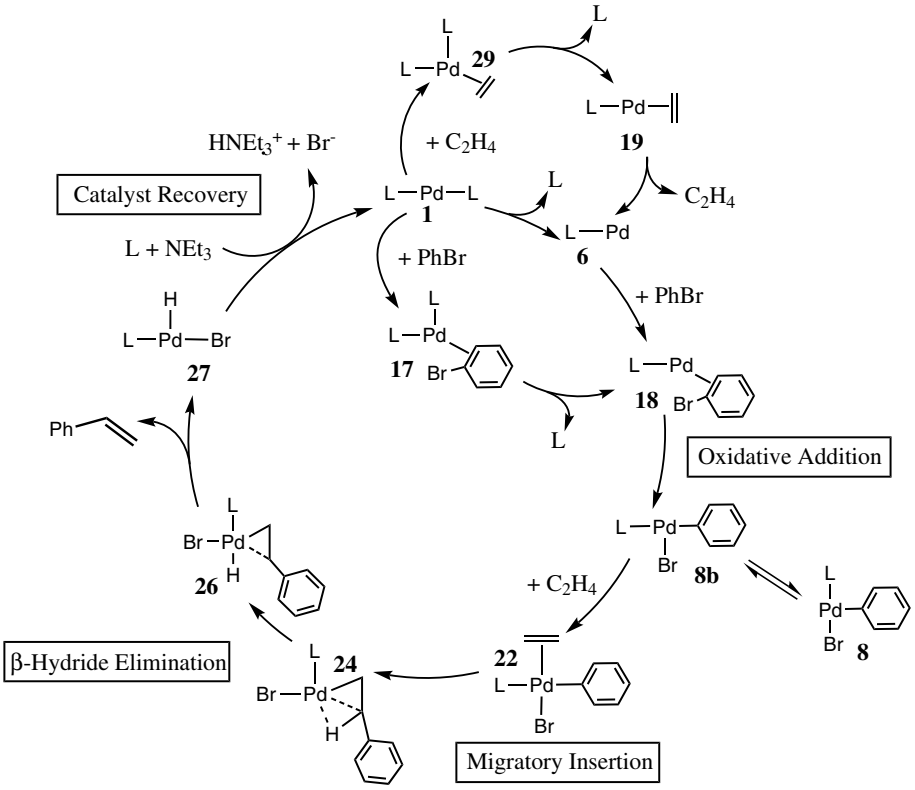

Scheme 4. Neutral mechanism of the Heck reaction for palladium with monophosphine ligands (L).

complexes. Issues related to the palladium nanoparticles and "ligand free" palladium as intermediates [33,34,73,74] in the Heck reaction cycle will be examined in a future study.

Acknowledgements

We would like to thank the National Science Foundation (Grant No. CHE-0518074 and CHE-0541587), the Welch Foundation (Grant No. A-0648) and Royal Thai Government for financial support.

Appendix A. Supplementary material

Supplementary data associated with this article can be found, in the online version, at doi:10.1016/j.jorganchem.2008.01.034.

References

[1] R.F. Heck, J.P. Nolley, Org. Chem. 37 (1972) 2320–2322.
[2] T. Mizoroki, K. Mori, A. Ozaki, Bull. Chem. Soc. Jpn. 44 (1971) 581.
[3] K. Sakoda, J. Mihara, J. Ichikawa, Chem. Commun. (2005) 4684–4686.
[4] L.A. Arnold, W. Luo, R.K. Guy, Org. Lett. 6 (2004) 3005–3007.
[5] A.B. Dounay, L.E. Overman, A.D. Wrobleski, J. Am. Chem. Soc. 127 (2005) 10186–10187.
[6] J. Mo, L. Xu, J. Ruan, S. Liu, J. Xiao, Chem. Commun. (2006) 3591–3593.
[7] T. Tu, X.-L. Hou, L.-X. Dai, Org. Lett. 5 (2003) 3651–3653.
[8] B. Mariampillai, C. Herse, M. Lautens, Org. Lett. 7 (2005) 4745–4747.
[9] B. Schmidt, Chem. Commun. (2003) 1656–1657.
[10] A.d. Meijere, F.E. Meyer, Angew. Chem., Int. Ed. 33 (2004) 2379–2411.
[11] I.P. Beletskaya, A.V. Cheprakov, Chem. Rev. 100 (2000) 3009–3066.
[12] A.M. Trzeciak, J.J. Ziołkowski, Coord. Chem. Rev. 251 (2007) 1281–1293.
[13] L. Yin, J. Liebscher, Chem. Rev. 107 (2007) 133–173.
[14] N.T.S. Phan, M.V.D. Sluys, C.W. Jones, Adv. Synth. Catal. 348 (2006) 609–679.
[15] R.B. Bedford, C.S.J. Cazin, D. Holder, Coord. Chem. Rev. 248 (2004) 2283–2321.
[16] A.M. Trzeciak, J.J. Ziołkowski, Coord. Chem. Rev. 249 (2005) 2308–2322.
[17] V. Farina, Adv. Synth. Catal. 346 (2004) 1553–1582.
[18] U. Christmann, R. Vilar, Angew. Chem., Int. Ed. 44 (2005) 366–374.
[19] A.F. Littke, G.C. Fu, Angew. Chem., Int. Ed. 41 (2002) 4126–4211.
[20] N.J. Witcombe, K.K. Hii, S.E. Gibson, Tetrahedron 57 (2001) 7449–7476.
[21] J.P. Knowles, A. Whiting, Org. Biomol. Chem. 5 (2007) 31–44.
[22] W. Cabri, I. Candiani, Acc. Chem. Res. 28 (1995) 2–7.
[23] A.F. Littke, G.C. Fu, J. Org. Chem. 64 (1999) 10–11.
[24] K.H. Shaughnessy, P. Kim, J.F. Hartwig, J. Am. Chem. Soc. 121 (1999) 2123–2132.
[25] A. Ehrentraut, A. Zapf, M. Beller, Synlett (2000) 1589–1592.
[26] M. Portnoy, Y. Ben-David, I. Rousso, D. Milstein, Organometallics 13 (1994) 3465–3479.
[27] M. Ohff, A. Ohff, M.E. van der Boom, D. Milstein, J. Am. Chem. Soc. 119 (1997) 11687–11688.
[28] D. Morales-Morales, R. Redón, C. Yung, C.M. Jensen, Chem. Commun. (2000) 1619–1620.
[29] W.A. Herrmann, M. Elison, J. Fischer, C. Köcher, G.R.J. Artus, Angew. Chem., Int. Ed. 34 (1995) 2371–2374.
[30] T. Weskamp, V.P.W. Böhm, W.A. Herrmann, J. Organomet. Chem. 585 (2001) 348–352.
[31] R.B. Bedford, Chem. Commun. (2003) 1787–1796.
[32] D.E. Bergbreiter, P.L. Osburn, Y.-S. Liu, J. Am. Chem. Soc. 121 (1999) 9531–9538.
[33] A.H.M.d. Vries, F.J. Parlevliet, L.S.-v.d. Vondervoort, J.H.M. Mommers, H.J.W. Henderickx, M.A.M. Walet, J.G.d. Vries, Adv. Synth. Catal. 344 (2002) 996–1002.
[34] A.H.M.d. Vries, J.M.C.A. Mulders, J.H.M. Mommers, H.J.W. Henderickx, J.G.d. Vries, Org. Lett. 5 (2003) 3285–3288.
[35] D.G. Blackmond, T. Schultz, J.S. Mathew, C. Loew, T. Rosner, A. Pfaltz, Synlett 18 (2006) 3135–3139.
[36] C. Amatore, F. Pfluger, Organometallics 9 (1990) 2276–2282.
[37] J.-F. Fauvarque, F. Pfluger, M. Troupel, J. Organomet. Chem. 208 (1981) 419–427.
[38] A.F. Littke, C.Y. Dai, G.C. Fu, J. Am. Chem. Soc. 122 (2000) 4020.
[39] J.P. Stambuli, M. Buhl, J.F. Hartwig, J. Am. Chem. Soc. 124 (2002) 9346–9347.
[40] J.P. Stumbuli, C.D. Incarvito, M. Buehl, J.F. Hartwig, J. Am. Chem. Soc. 126 (2004) 1184–1194.
[41] K. Kiewel, Y. Liu, D.E. Bergbreiter, G.A. Sulikowski, Tetrahedron Lett. 40 (1999) 8945–8948.
[42] C. Amatore, E. Carre', A. Jutand, Y. Medjour, Organometallics 21 (2002) 4540–4545.
[43] E.G. Samsel, J.R. Norton, J. Am. Chem. Soc. 106 (1984) 5505–5512.
[44] K.J. Cavell, Coord. Chem. Rev. 155 (1996) 209–243.
[45] D.L. Thorn, R. Hoffmann, J. Am. Chem. Soc. 100 (1978) 2079–2090.
[46] B.-L. Lin, L. Liu, Y. Fu, S.-W. Luo, Q. Chen, Q.-X. Guo, Organometallics 23 (2004) 2114–2123.
[47] W. Cabri, I. Candiani, A. Bedeschi, S. Penco, J. Org. Chem. 57 (1992) 1481–1486.
[48] K. Albert, P. Gisdakis, N. Rösch, Organometallics 17 (1998) 1608–1616.
[49] A. Sundermann, O. Uzan, J.M.L. Martin, Chem. Eur. J. 7 (2001) 1703–1711.
[50] H.M. Senn, T. Ziegler, Organometallics 23 (2004) 2980–2988.
[51] L.J. Goossen, D. Koley, H. Hermann, W. Thiel, Chem. Commun. (2004) 2141–2143.
[52] L.J. Goossen, D. Koley, H.L. Hermann, W. Thiel, Organometallics 24 (2005) 2398–2410.
[53] M. Ahlquist, P.-O. Norrby, Organometallics 26 (2007) 550–553.
[54] M. Ahlquist, P. Fristrup, D. Tanner, P.-O. Norrby, Organometallics 25 (2006) 2066–2073.
[55] M.J. Frisch, G.W. Trucks, H.B. Schlegel, G.E. Scuseria, M.A. Robb, J.R. Cheeseman, J.A. Montgomery Jr., T. Vreven, K.N. Kudin, J.C. Burant, J.M. Millam, S.S. Iyengar, J. Tomasi, V. Barone, B. Mennucci, M. Cossi, G. Scalmani, N. Rega, G.A. Petersson, H. Nakatsuji, M. Hada, M. Ehara, K. Toyota, R. Fukuda, J. Hasegawa, M. Ishida, T. Nakajima, Y. Honda, O. Kitao, H. Nakai, M. Klene, X. Li, J.E. Knox, H.P. Hratchian, J.B. Cross, C. Adamo, J. Jaramillo, R. Gomperts, R.E. Stratmann, O. Yazyev, A.J. Austin, R. Cammi, C. Pomelli, J.W. Ochterski, P.Y. Ayala, K. Morokuma, G.A. Voth, P. Salvador, J.J. Dannenberg, V.G. Zakrzewski, S. Dapprich, A.D. Daniels, M.C. Strain, O. Farkas, D.K. Malick, A.D. Rabuck, K. Raghavachari, J.B. Foresman, J.V. Ortiz, Q. Cui, A.G. Baboul, S. Clifford, J. Cioslowski, B.B. Stefanov, G. Liu, A. Liashenko, P. Piskorz, I. Komaromi, R.L. Martin, D.J. Fox, T. Keith, M.A. Al-Laham, C.Y. Peng, A. Nanayakkara, M. Challacombe, P.M.W. Gill, B. Johnson, W. Chen, M.W. Wong, C. Gonzalez, J.A. Pople, Gaussian 03, Gaussian, Inc., Pittsburgh, PA, 2003.
[56] J.P. Perdew, K. Burke, M. Ernzerhof, Phys. Rev. Lett. 77 (1996) 3865–3868.
[57] P.J. Hay, W.R. Wadt, J. Chem. Phys. 82 (1985) 270–283.
[58] P.J. Hay, W.R. Wadt, J. Chem. Phys. 82 (1985) 299–310.
[59] M. Couty, M.B. Hall, J. Comput. Chem. 17 (1996) 1359–1370.
[60] P.C. Hariharan, J.A. Pople, Theor. Chim. Acta 28 (1973) 213–222.
[61] G.A. Petersson, M.A. Al-Laham, J. Chem. Phys. 94 (1991) 6081–6090.

[62] G.A. Petersson, A. Bennett, T.G. Tensfeldt, M.A. Al-Laham, W.A. Shirley, J. Mantzaris, J. Chem. Phys. 89 (1988) 2193–2218.
[63] G.T.d. Jong, D.P. Geerke, A. Diefenbach, F.M. Bickelhaupt, Chem. Phys. 313 (2005) 261–270.
[64] A.D. Becke, J. Chem. Phys. 98 (1993) 5648.
[65] C. Lee, W. Yang, R.G. Parr, Phys. Rev. B 37 (1988) 785.
[66] V. Barone, M. Cossi, J. Phys. Chem. A 102 (1998) 1995.
[67] M. Cossi, N. Rega, G. Scalmani, V. Barone, J. Comput. Chem. 24 (2003) 669–681.
[68] S. Wan, R.H. Stote, M. Karplus, J. Chem. Phys. 121 (2004) 9539.
[69] When we optimize $Pd(PH_3)_2$ without density fitting function and tighten the cutoffs in the convergence criteria, the P–Pd–P angle is 179.5°.
[70] J.M. Brown, N.A. Cooley, Organometallics 9 (1990) 353.
[71] E. Rincon, A. Toro-Labbe, Chem. Phys. Lett. 438 (2007) 93.
[72] A.L. Casado, P. Espinet, Organometallics 17 (1998) 954–959.
[73] M.T. Reetz, E. Westermann, Angew. Chem., Int. Ed. 39 (2000) 165–168.
[74] J.G.d. Vries, Dalton Trans. (2006) 421–429.